

Robust path-following control for articulated heavy-duty vehicles

Filipe Marques Barbosa^a, Lucas Barbosa Marcos^a, Maíra Martins da Silva^b, Marco Henrique Terra^a,
Valdir Grassi Junior^{a,*}

^a*Department of Electrical and Computer Engineering, São Carlos School of Engineering, University of São Paulo, São Carlos, Brazil*

^b*Department of Mechanical Engineering, São Carlos School of Engineering, University of São Paulo, São Carlos, Brazil*

Abstract

Path following and lateral stability are crucial issues for autonomous vehicles. Moreover, these problems increase in complexity when handling articulated heavy-duty vehicles due to their poor manoeuvrability, large sizes and mass variation. In addition, uncertainties on mass may have the potential to significantly decrease the performance of the system, even to the point of destabilising it. These parametric variations must be taken into account during the design of the controller. However, robust control techniques usually require offline adjustment of auxiliary tuning parameters, which is not practical, leading to sub-optimal operation. Hence, this paper presents an approach to path-following and lateral control for autonomous articulated heavy-duty vehicles subject to parametric uncertainties by using a robust recursive regulator. The main advantage of the proposed controller is that it does not depend on the offline adjustment of tuning parameters. Parametric uncertainties were assumed to be on the payload, and an \mathcal{H}_∞ controller was used for performance comparison. The performance of both controllers is evaluated in a double lane-change manoeuvre. Simulation results showed that the proposed method had better performance in terms of robustness, lateral stability, driving smoothness and safety, which demonstrates that it is a very promising control technique for practical applications.

Keywords: articulated vehicle; path following; lateral control; robust control; heavy-duty vehicle

1. Introduction

The advantages of autonomous vehicles are well-established in the academic literature. For example, reducing the number of accidents; easing the transportation of elderly and disabled people [1]; offering more profitable means of transportation to industries and more efficient transportation methods to the military [2, 3]; improving ride comfort for passengers [4]; increasing road utilisation [5], etc.

Nowadays, heavy load vehicles are responsible for much of cargo transportation. The use of articulated heavy vehicles has been increasing due to their economic advantages [6], freight transportation efficiency [7] and the growing demand for high capacity transport vehicles [8]. Furthermore, the same technologies used for autonomous cars can also be addressed to articulated heavy-duty vehicles [9], additionally increasing productivity and reducing cargo transportation costs [10].

In the literature, different control techniques have been used to solve the path-following problem for autonomous vehicles. Alcalá *et al.* [11] used a Lyapunov-based technique with linear quadratic regulator - linear matrix inequality (LQR-LMI) tuning to solve the problem of guidance in an autonomous vehicle. Ji *et al.* [12] proposed a robust steering controller based on a backstepping variable structured control to

*Correspondence to: Department of Electrical and Computer Engineering, São Carlos School of Engineering, University of São Paulo, Av. Trabalhador São-carlense 400, 13566-590, São Carlos, SP, Brazil

Email addresses: marquesfilipeb@gmail.com (Filipe Marques Barbosa), lucasbmarcos@usp.br (Lucas Barbosa Marcos), mairams@sc.usp.br (Maíra Martins da Silva), terra@sc.usp.br (Marco Henrique Terra), vgrassi@usp.br (Valdir Grassi Junior)

maintain the yaw stability and minimise the lateral error. Mitraji *et al.* [13] designed and implemented an adaptive Second Order Sliding Mode Control for a four wheels Skid-Steered Mobile Robot. The objective was to follow a predefined trajectory in the presence of disturbance and parametric uncertainties. Chu *et al.* [14] applied an active disturbance rejection control to a steering controller design with the aim to guarantee the lane keeping of the vehicle in the presence of uncertainties and external disturbance. Lastly, Hu *et al.* [15] presented an \mathcal{H}_∞ output-feedback control strategy based on the mixed genetic algorithms and linear matrix inequality to perform the path following of autonomous ground vehicles.

In addition, some authors have proposed the use of an active trailer steering system to improve path following and attitude control of articulated vehicles [7, 16, 17]. For instance, different vehicle conditions have been considered by Guan *et al.* [17] for deriving a model predictive control strategy. Regarding autonomous articulated vehicles, some control design strategies have been exploited in the literature. Yuan *et al.* [18] proposed a lateral-longitudinal control scheme using automatic steering strategies to avoid jackknifing, considering input limitations. Michałek [19] presented a highly scalable nonlinear cascade-like control to solve the path-following problem for articulated robotic vehicles equipped with arbitrary number of off-axle hitched trailers. With respect to the path-following problem for articulated vehicles, an active steering controller of the tractor and trailer based on LQR was designed by Kim *et al.* [16], whilst a novel sliding mode controller was proposed by Nayl *et al.* [20]. However, the autonomous control of articulated heavy-duty vehicles remains an issue. As payload may be much greater than vehicle weight itself [6], mass is a critical parameter in vehicle dynamics and those vehicles are especially affected by mass variations. Hence, a control technique that overcomes the parametric uncertainties in the vehicle model is necessary, and it ensures system stability and performance objectives for a range of parameter values [6]. This leads to the need of robust controllers designed to withstand mass variations.

Kati *et al.* [6] proposed an \mathcal{H}_∞ controller to deal with uncertainties on payload of the vehicle. However, the \mathcal{H}_∞ controller depends on the offline adjustment of the auxiliary parameter γ for each payload value. This results in sub-optimal controller operation because it is not practical to adjust γ every time the payload varies. In order to address this problem, the contribution of this paper is a novel approach for the lateral control of an autonomous articulated heavy-duty vehicle, based on a Robust Linear Quadratic Regulator (RLQR) presented in [21] and [22]. The main advantage of the proposed controller is that it does not require any auxiliary tuning parameters, which is useful for online applications. A continuous-time model for the articulated vehicle in state-space form is presented. Then, the model is discretised in order to apply discrete RLQ control for solving a path-following problem.

Since \mathcal{H}_∞ control is widely used for path-tracking problems [15] and for robustifying the control strategy in automotive applications [23, 24], a standard \mathcal{H}_∞ controller is also applied to the same plant for the sake of comparison. Uncertainties on vehicle mass are introduced, then the performance of both controllers is compared in different cases. Simulation tests evaluate robustness, steering behaviour, truck displacement error and orientation error.

The RLQR ensures stability for a range of possible payloads. On the other hand, the \mathcal{H}_∞ controller is dependent on the auxiliary parameter γ . Therefore, it cannot maintain good performance (or even stability) for a wide range of payloads, unless γ is adjusted offline [21].

The paper is organised as follows: Section 2 presents both the model of a heavy articulated vehicle in continuous-time state-space form and a path-following model, which are properly put together to make a single model; Section 3 exhibits the RLQR, showing how it is derived from a quadratic cost function and a robust regularised least squares problem; Section 4 shows and discusses the application of the RLQR and its results compared to an \mathcal{H}_∞ controller; Section 5 brings the conclusions.

2. System modelling

With the aim to make the articulated heavy-duty vehicle follow a desired path, it is not only necessary to minimise the lateral offset and heading error, but also ensure the vehicle stability. Therefore, the system modelling must take into account the path following and dynamic variables. This section introduces the vehicle model for simulations and control design.

2.1. Path-following model

In order to solve the path-following problem, the lateral controller aims to reduce lateral displacement and orientation angle errors of the towing vehicle. Therefore, the path-following model adopted here is based on the equations presented by Skjetne and Fossen [25]. Fig. 1 shows the schematic diagram of path-following model for an articulated vehicle, where \dot{y}_1 is tractor lateral velocity and v is tractor longitudinal velocity. The lateral displacement of the vehicle to a given reference path is the distance ρ from tractor centre of gravity to the closest point D on the desired path. The tractor orientation error is defined as $\theta = \psi_1 - \psi_{des}$, where ψ_1 and ψ_{des} are the current and desired orientation angles of the tractor, respectively.

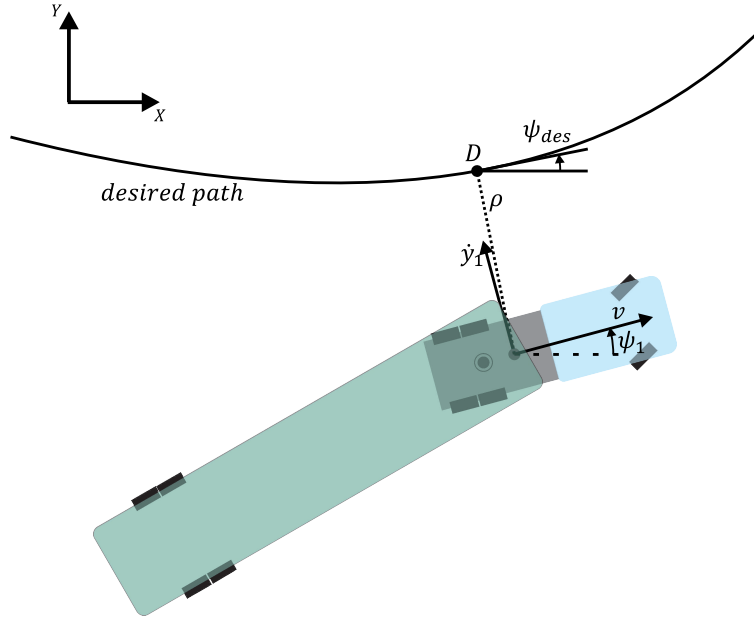


Figure 1: Schematic diagram for path-following model.

Based on Serret-Frenet equations [25], the path-following model of the autonomous ground vehicle is expressed as

$$\begin{aligned}\dot{\rho} &= v \sin \theta + \dot{y}_1 \cos \theta \\ \dot{\theta} &= \dot{\psi}.\end{aligned}\tag{1}$$

The displacement error ρ can be rewritten in the linear form by assuming that the orientation error θ is small, as follows

$$\dot{\rho} = v\theta + \dot{y}_1.\tag{2}$$

2.2. Articulated vehicle model

Single-track models are widely used in literature [11, 12, 7, 6] to describe the vehicle lateral behaviour without much modelling and parametrisation effort [26]. These assume that the vehicle can be described by only one equivalent track in each axle, linked by the vehicle body. Consequently, it only takes into account the planar movement of the vehicle, disregarding roll and pitch effects. The nonholonomic linear model adopted here is based on bicycle model presented by van de Molengraft-Luijten *et al.* [27].

Fig. 2 shows the free body diagram of a vehicle with one articulation, where the following assumptions are adopted:

- Differences between left and right track are ignored;
- Vehicle velocity parameter is constant;

- The mass of each unit is assumed to be concentrated at the centre of gravity;
- Lateral tyre forces are proportional to the tyre slip angles;
- There is no load transfer.

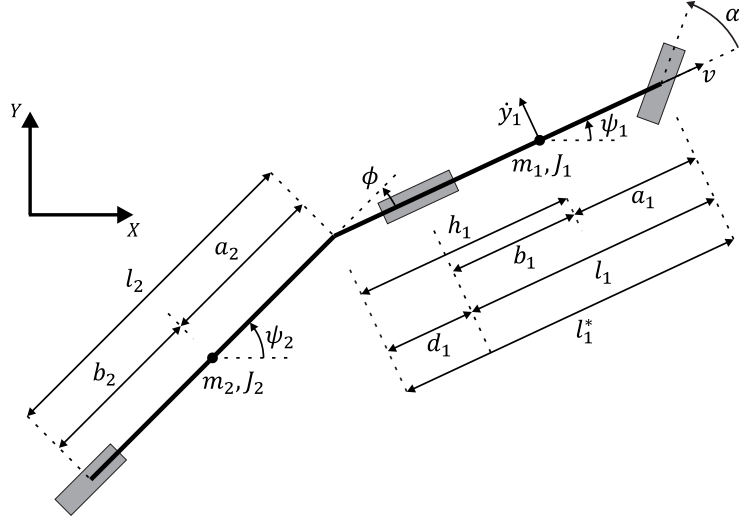


Figure 2: Articulated vehicle single-track model.

Table 1 details the parameters of the articulated vehicle shown in Fig. 2. Note that hitch point may be positioned behind the towing vehicle rear axle (e.g. truck-full trailers where $h_1 > b_1$ and $d_1 > 0$) or in front of it (e.g. tractor-semitrailers where $h_1 < b_1$ and $d_1 < 0$).

Table 1: Description of vehicle parameters

Parameter	Meaning	Unit
a_1	Distance from the front axle to the tractor centre of gravity	m
a_2	Distance from the coupling point to the trailer centre of gravity	m
b_1	Distance from the tractor rear axle to the tractor centre of gravity	m
b_2	Distance from the trailer axle to the trailer centre of gravity	m
l_1	Tractor wheelbase	m
l_2	Trailer wheelbase	m
d_1	The distance between the tractor rear axle and the coupling point	m
h_1	The distance between coupling point and the tractor centre of gravity	m
l_1^*	The distance between the tractor front axle and the coupling point	m
v	Forward velocity	m/s
\dot{y}_1	Lateral Velocity	m/s
m_1	Tractor mass	kg
m_2	Trailer mass	kg
J_1	Tractor moment of inertia	$kg\ m^2$
J_2	Trailer moment of inertia	$kg\ m^2$
ψ_1	Tractor yaw	rad
ψ_2	Trailer yaw	rad
α	Steering angle	rad
ϕ	Articulation angle	rad

In order to improve the path following, lateral displacement ρ and orientations error θ must be as small as possible. In addition, it is necessary to ensure vehicle stability. Hence, the lateral velocity \dot{y}_1 , yaw rate $\dot{\psi}_1$, articulation angle rate $\dot{\phi}$ and articulation angle ϕ must be well controlled.

The motion equation of the articulated vehicle can be expressed as

$$M\dot{x} = Ax + B\alpha, \quad (3)$$

with the state vector defined as $x = [\dot{y}_1, \dot{\psi}_1, \dot{\phi}, \phi, \rho, \theta]^T$. Therefore, the state-space description of the path-following model for the articulated heavy-duty vehicle is written as

$$\begin{bmatrix} m_1 + m_2 & -m_2(h_1 + a_2) & -m_2a_2 & 0 & 0 & 0 \\ -m_2h_1 & J_1 + m_2h_1(h_1 + a_2) & m_2h_1a_2 & 0 & 0 & 0 \\ -m_2a_2 & J_2 + m_2a_2(h_1 + a_2) & J_2 + m_2a_2^2 & 0 & 0 & 0 \\ 0 & 0 & 0 & 1 & 0 & 0 \\ 0 & 0 & 0 & 0 & 1 & 0 \\ 0 & 0 & 0 & 0 & 0 & 1 \end{bmatrix} \dot{x} = \begin{bmatrix} \frac{-c_1 - c_2 - c_3}{v} & \frac{c_3(h_1 + l_2) - a_1c_1 + b_1c_2 - (m_1 + m_2)v^2}{v} & \frac{c_3l_2}{v} & c_3 & 0 & 0 \\ \frac{c_3h_1 - a_1c_1 + b_1c_2}{v} & \frac{m_2h_1v^2 - a_1^2c_1 - b_1^2c_2 - c_3h_1(h_1 + l_2)}{v} & \frac{-c_3h_1l_2}{v} & -c_3h_1 & 0 & 0 \\ \frac{c_3l_2}{v} & \frac{m_2a_2v^2 - c_3l_2(h_1 + l_2)}{v} & \frac{-c_3l_2^2}{v} & -c_3l_2 & 0 & 0 \\ 0 & 0 & 1 & 0 & 0 & 0 \\ 1 & 0 & 0 & 0 & 0 & v \\ 0 & 1 & 0 & 0 & 0 & 0 \end{bmatrix} x + \begin{bmatrix} c_1 \\ a_1c_1 \\ 0 \\ 0 \\ 0 \\ 0 \end{bmatrix} \alpha, \quad (4)$$

where the vehicle steering angle α is the control input, c_1 , c_2 and c_3 are the cornering stiffness of the tractor front axle, tractor rear axle and trailer axle, respectively.

Fancher demonstrated in [28] (as cited in [29]) that the relation between the tyre cornering stiffness and the vertical load forces are approximately linear for truck tyres. Thus, a normalised cornering stiffness f_j is used, and the cornering stiffness c_j scales linearly with the vertical load force of the axle F_{z_j} . The cornering stiffness parameters are calculated as

$$c_j = f_j F_{z_j} \text{ with } j = 1, \dots, p, \quad (5)$$

where p is the number of axles in the vehicle, $j = 1$ corresponds to the tractor front axle, $j = 2$ to the tractor rear axle and $j = 3$ to the trailer axle.

The vertical force in each axle can be calculated as

$$\begin{aligned} F_{z_1} &= m_1g \frac{b_1}{l_1} - m_2g \frac{b_2d_1}{l_2l_1} \\ F_{z_2} &= m_1g \frac{a_1}{l_1} + m_2g \frac{b_2l_1^*}{l_2l_1} \\ F_{z_3} &= m_2g \frac{a_2}{l_2}, \end{aligned} \quad (6)$$

where g is the gravitational acceleration. Moreover, Houben [30] (as cited in [27]) observed that the normalised cornering stiffness of trailer tyres, drive and steer are approximately the same. Therefore, it is assumed $f_1 \approx f_2 \approx f_3$.

Nevertheless, a discrete state-space representation of the system is necessary in order to perform the robust recursive control for time-varying linear systems subject to parametric uncertainties. Hence, the system (4) is discretised by using the Tustin method.

3. Robust recursive regulator

The goal of the Robust Linear Quadratic Regulator (RLQR) is to minimise a given cost function subject to the maximum influence of parametric uncertainties. It is made by implementing an optimal feedback law

in the form $u_i = K_i x_i$, where K_i is the feedback gain. This section describes the robust recursive regulator presented by Terra *et al.* in [21] and Cerri *et al.* in [22].

3.1. Problem formulation

Consider the following discrete-time linear system subject to parametric uncertainties

$$x_{i+1} = (F_i + \delta F_i)x_i + (G_i + \delta G_i)u_i, \quad (7)$$

where $i = 0, \dots, N$, $x_i \in \mathbb{R}^n$ is the state vector, $u_i \in \mathbb{R}^m$ is the control input, and $F_i \in \mathbb{R}^{n \times n}$ and $G_i \in \mathbb{R}^{n \times m}$ are known nominal model matrices. Uncertainty matrices δF_i and δG_i represent parametric uncertainties modelled as

$$[\delta F_i \quad \delta G_i] = H_i \Delta_i [E_{F_i} \quad E_{G_i}], \quad (8)$$

where $i = 0, \dots, N$; $H_i \in \mathbb{R}^{n \times p}$; $E_{F_i} \in \mathbb{R}^{l \times n}$ and $E_{G_i} \in \mathbb{R}^{l \times m}$ are known matrices; and $\Delta_i \in \mathbb{R}^{p \times l}$ is an arbitrary matrix such that $\|\Delta_i\| \leq 1$.

In order to obtain the Robust Linear Quadratic Regulator, the following optimisation problem must be solved [21]:

$$\min_{x_{i+1}, u_i} \max_{\delta F_i, \delta G_i} \bar{J}_i^\mu(x_{i+1}, u_i, \delta F_i, \delta G_i), \quad (9)$$

where \bar{J}_i^μ is the cost function

$$\begin{aligned} \bar{J}_i^\mu(x_{i+1}, u_i, \delta F_i, \delta G_i) = \\ \begin{bmatrix} x_{i+1} \\ u_i \end{bmatrix}^T \begin{bmatrix} P_{i+1}^r & 0 \\ 0 & R_i \end{bmatrix} \begin{bmatrix} x_{i+1} \\ u_i \end{bmatrix} + \Phi^T \begin{bmatrix} Q_i & 0 \\ 0 & \mu I \end{bmatrix} \Phi, \end{aligned} \quad (10)$$

with fixed penalty parameter $\mu > 0$, weighing matrices $Q_i \succ 0$, $R_i \succ 0$, $P_{i+1} \succ 0$ and

$$\Phi = \left\{ \begin{bmatrix} 0 & 0 \\ I & -G_i - \delta G_i \end{bmatrix} \begin{bmatrix} x_{i+1} \\ u_i \end{bmatrix} - \begin{bmatrix} -I \\ F_i + \delta F_i \end{bmatrix} x_i \right\}.$$

Details on penalty function can be seen in [22].

Remark. The optimisation problem (9)-(10) is a particular case of the robust least-squares problem and will be treated below.

3.2. Regularised least squares

Consider the least-square minimisation problem defined by

$$\min_{x \in \mathbb{R}^m} \{J(x)\}, \quad (11)$$

where $J(x)$ is a regularised quadratic functional

$$\begin{aligned} J(x) &= \|x\|_Q^2 + \|Ax - b\|_W^2 \\ &= x^T Q x + (Ax - b)^T W (Ax - b), \end{aligned} \quad (12)$$

with $Q \in \mathbb{R}^{m \times m}$ (regularisation matrix) and $W \in \mathbb{R}^{m \times n}$ symmetric positive definite, $A \in \mathbb{R}^{n \times n}$ and $b \in \mathbb{R}^n$ known, and $x \in \mathbb{R}^m$ the unknown vector.

Lemma 3.1. The optimal solution for the problem (11)-(12) is

$$x^* = (Q + A^T W A)^{-1} A^T W b.$$

Proof. See [31]. □

3.3. Robust regularised least-squares problem

In the regularised least-squares problem established in (11)-(12), now suppose that the matrix A and the vector b are under influence of uncertainties δA and δb , respectively. Consider the min-max optimisation problem defined in [32] in the form:

$$\min_x \max_{\delta A, \delta b} \{J(x, \delta A, \delta b)\}, \quad (13)$$

with $J(x, \delta A, \delta b)$ given by

$$J(x, \delta A, \delta b) = \|x\|_Q^2 + \|(A + \delta A)x - (b + \delta b)\|_W^2, \quad (14)$$

and the uncertainties δA and δb modelled as

$$\begin{bmatrix} \delta A & \delta b \end{bmatrix} = H\Delta \begin{bmatrix} E_A & E_b \end{bmatrix}, \quad (15)$$

with A, b, H, E_A, E_b, Q and W known matrices, Δ a contraction arbitrary matrix ($\|\Delta\| \leq 1$) and x an unknown vector. The optimal solution for the problem (13)-(15) is given below. See demonstration details in [32], where a general result is proposed.

Lemma 3.2. *The optimisation problem (13)-(15) has a unique solution*

$$x^* = \left(\hat{Q} + A^T \hat{W} A \right)^{-1} \left(A^T \hat{W} b + \hat{\lambda} E_A^T E_b \right),$$

with \hat{Q} and \hat{W} defined as

$$\begin{aligned} \hat{Q} &:= Q + \hat{\lambda} E_A^T E_A, \\ \hat{W} &:= W + WH(\hat{\lambda} I - H^T WH)^\dagger H^T W. \end{aligned}$$

The non-negative scalar parameter obtained from the minimisation problem

$$\hat{\lambda} = \arg \min_{\lambda \geq \|H^T WH\|} \{\Gamma(\lambda)\},$$

where $\Gamma(\lambda) := \|x(\lambda)\|_Q^2 + \lambda \|E_A x(\lambda) - E_b\|^2 + \|Ax(\lambda) - b\|_{W(\lambda)}^2$ with

$$\begin{aligned} Q(\lambda) &:= Q + \lambda E_A^T E_A, \\ \tilde{Q}(\lambda) &:= Q(\lambda) + A^T W(\lambda) A, \\ W(\lambda) &:= W + WH(\lambda I - H^T WH)^\dagger H^T W, \\ x(\lambda) &:= \tilde{Q}(\lambda)^{-1} (A^T W(\lambda) b + \lambda E_A^T E_b). \end{aligned}$$

Proof. See [32] □

For this type of problem, it is appropriate to redefine Lemma 3.2 in terms of an array of matrices. The following lemma shows an optimal solution for the problem (13)-(15) in an alternative structure to this fundamental theorem.

Lemma 3.3. *Suppose $Q \succ 0$ and $W \succ 0$. The solution x^* for the problem (13)-(15) can be rewritten as*

$$\begin{bmatrix} x^* \\ J(x^*) \end{bmatrix} = \begin{bmatrix} 0 & 0 \\ 0 & b \\ 0 & E_b \\ I & 0 \end{bmatrix}^T \begin{bmatrix} Q^{-1} & 0 & 0 & I \\ 0 & \hat{W}^{-1} & 0 & A \\ 0 & 0 & \hat{\lambda}^{-1} I & E_A \\ I & A^T & E_A^T & 0 \end{bmatrix}^{-1} \begin{bmatrix} 0 \\ b \\ E_b \\ 0 \end{bmatrix},$$

with \hat{W} and $\hat{\lambda}$ as in Lemma 3.2.

Proof. See [22]. □

3.4. Robust Linear Quadratic Regulator

The optimisation problem (9)-(10) is solved based on the solution of a general robust regularised least-squares problem [21]. Back to the solution presented in Lemma 3.2, with $\mu > 0$, the RLQR has an optimal operation point for each step k of the algorithm. When suitable identifications of (9)-(10) with (13)-(15) are carried out, the regularisation of the robust regulator is reached thanks to minimisation over both $x_{i+1}(\mu)$ and $u_i(\mu)$ [21]:

$$\begin{aligned}
Q &\leftarrow \begin{bmatrix} P_{i+1} & 0 \\ 0 & R_i \end{bmatrix}, \quad x \leftarrow \begin{bmatrix} x_{i+1}(\mu) \\ u_k(\mu) \end{bmatrix}, \quad W \leftarrow \begin{bmatrix} Q_i & 0 \\ 0 & \mu I \end{bmatrix}, \\
A &\leftarrow \begin{bmatrix} 0 & 0 \\ I & -G_i \end{bmatrix}, \quad \delta A \leftarrow \begin{bmatrix} 0 & 0 \\ 0 & -\delta G_i \end{bmatrix}, \quad \Delta \leftarrow \Delta_i \\
b &\leftarrow \begin{bmatrix} -I \\ F_i \end{bmatrix} x_i, \quad \delta b \leftarrow \begin{bmatrix} 0 \\ \delta F_i \end{bmatrix} x_i, \\
H &\leftarrow \begin{bmatrix} 0 \\ H_i \end{bmatrix}, \quad E_A \leftarrow [0 -E_{G_i}], \quad E_b \leftarrow E_{F_i} x_i,
\end{aligned} \tag{16}$$

The following lemma shows a framework given in terms of an array of matrices with the purpose of calculating the optimal cost function, control input and state trajectory.

Theorem 3.1. *For each $\mu > 0$ in the optimisation problem (9)-(10), the optimal solution is given by*

$$\begin{bmatrix} x_{i+1}^*(\mu) \\ u_i^*(\mu) \\ \tilde{J}_i^\mu(x_{i+1}^*(\mu), u_i^*(\mu)) \end{bmatrix} = \begin{bmatrix} I & 0 & 0 \\ 0 & I & 0 \\ 0 & 0 & x_i(\mu)^T \end{bmatrix}^T \begin{bmatrix} L_{i,\mu} \\ K_{i,\mu} \\ P_{i,\mu} \end{bmatrix} x_i, \tag{17}$$

where the closed-loop system matrix L_i and the feedback gain K_i result from the recursion

$$\begin{bmatrix} L_i \\ K_i \\ P_i \end{bmatrix} = \begin{bmatrix} 0 & 0 & -I & \mathcal{F}_i & 0 & 0 \\ 0 & 0 & 0 & 0 & 0 & I \\ 0 & 0 & 0 & 0 & I & 0 \end{bmatrix} \Xi^{-1} \begin{bmatrix} 0 \\ 0 \\ -I \\ \mathcal{F}_i \\ 0 \\ 0 \end{bmatrix}, \tag{18}$$

with

$$\Xi = \begin{bmatrix} P_{i+1}^{-1} & 0 & 0 & 0 & I & 0 \\ 0 & R_i^{-1} & 0 & 0 & 0 & I \\ 0 & 0 & Q_i^{-1} & 0 & 0 & 0 \\ 0 & 0 & 0 & \Sigma_i(\mu, \hat{\lambda}_i) & \mathcal{I} & -\mathcal{G}_i \\ I & 0 & 0 & \mathcal{I}^T & 0 & 0 \\ 0 & I & 0 & -\mathcal{G}^T & 0 & 0 \end{bmatrix},$$

$$\Sigma_i = \begin{bmatrix} \mu^{-1}I - \hat{\lambda}_i^{-1}H_iH_i^T & 0 \\ 0 & \hat{\lambda}_i^{-1}I \end{bmatrix},$$

$$\mathcal{I} = \begin{bmatrix} I \\ 0 \end{bmatrix}, \quad \mathcal{G}_i = \begin{bmatrix} G_i \\ E_{G_i} \end{bmatrix}, \quad \mathcal{F}_i = \begin{bmatrix} F_i \\ E_{F_i} \end{bmatrix},$$

where P_{i+1} is the solution of the associated Riccati Equation and $\lambda_i > \|\mu H_i^T H_i\|$. Furthermore, alternatively one has

$$\begin{aligned}
P_{i,\mu} &= L_{i,\mu}^T P_{i+1} L_{i,\mu} + K_{i,\mu} R_i K_{i,\mu} + Q_i + \\
&(\mathcal{I} L_{i,\mu} - \mathcal{G}_i K_{i,\mu} - \mathcal{F}_i)^T \Sigma_{i,\mu}^{-1} (\mathcal{I} L_{i,\mu} - \mathcal{G}_i K_{i,\mu} - \mathcal{F}_i) \succ 0.
\end{aligned} \tag{19}$$

Proof. It follows from [Lemma 3.3](#), identifications performed in (16) and results shown in [\[22\]](#). \square

[Table 2](#) shows the Robust Linear Quadratic Regulator obtained with [Lemma 3.2](#). The parameter μ is associated with system robustness. It is responsible for ensuring the RLQR regularisation and validity of the equality (7). For maximum robustness, $\mu \rightarrow \infty$ and consequently $\Sigma_i \rightarrow 0$.

Table 2: The Robust Linear Quadratic Regulator

<p>Uncertain model: Consider the model (7)-(8) and criterion (9)-(10) with known $F_i, G_i, E_{F_i}, E_{G_i}, Q_i \succ 0$, and $R_i \succ 0$ for all i.</p> <p>Initial conditions: Define x_0 and $P_{i,N} \succeq 0$.</p> <p>Step 1: (Backward) For all $i = N - 1, \dots, 0$, compute</p> $\begin{bmatrix} L_i \\ K_i \\ P_i \end{bmatrix} = \begin{bmatrix} 0 & 0 & 0 \\ 0 & 0 & 0 \\ 0 & 0 & -I \\ 0 & 0 & F_i \\ 0 & 0 & E_{F_i} \\ I & 0 & 0 \\ 0 & I & 0 \end{bmatrix}^T \begin{bmatrix} P_{i+1}^{-1} & 0 & 0 & 0 & 0 & I & 0 \\ 0 & R_i^{-1} & 0 & 0 & 0 & 0 & I \\ 0 & 0 & Q_i^{-1} & 0 & 0 & 0 & 0 \\ 0 & 0 & 0 & 0 & 0 & I & -G_i \\ 0 & 0 & 0 & 0 & 0 & 0 & -E_{G_i} \\ I & 0 & 0 & I & 0 & 0 & 0 \\ 0 & I & 0 & -G_i^T & -E_{G_i}^T & 0 & 0 \end{bmatrix}^{-1} \begin{bmatrix} 0 \\ 0 \\ -I \\ F_i \\ E_{F_i} \\ 0 \\ 0 \end{bmatrix}.$ <p>Step 2: (Forward) For each $i = 0, \dots, N - 1$, obtain</p> $\begin{bmatrix} x_{i+1}^* \\ u_i^* \end{bmatrix} = \begin{bmatrix} L_i \\ K_i \end{bmatrix} x_i^*,$ <p>with the total cost given by $J_r^* = x_0^T P_0 x_0$.</p>	
-----------------------------------------------------------------------------------------------------------------------------------------------------------------------------------------------------------------------------------------------------------------------------------------------------------------------------------------------------------------------------------------------------------------------------------------------------------------------------------------------------------------------------------------------------------------------------------------------------------------------------------------------------------------------------------------------------------------------------------------------------------------------------------------------------------------------------------------------------------------------------------------------------------------------------------------------------------------------------------------------------------------------------------------------------------------------------------------------------------------------------------------------------------------------------------------------------------------	--

For each iteration of (19), the matrix $P_{i,\mu}$ is finite and $\mathcal{I}L_{i,\mu} - \mathcal{G}_i K_{i,\mu} - \mathcal{F}_i \rightarrow 0$, as shown in [\[21\]](#). Therefore,

$$\begin{aligned} L_{i,\infty} &= F_i + G_i K_{i,\infty} \\ E_{F_i} + E_{G_i} K_{i,\infty} &= 0, \end{aligned} \tag{20}$$

and a sufficient condition that satisfy (20) is

$$\text{rank} \left(\begin{bmatrix} E_{F_i} & E_{G_i} \end{bmatrix} \right) = \text{rank} (E_{G_i}). \tag{21}$$

Details about convergence and stability analysis can be found in [\[21\]](#).

4. Numerical results and discussion

For the controller validation, the RLQR was performed and compared with the \mathcal{H}_∞ controller in various operational conditions. The Matlab/Simulink simulation software was used for this purpose. Simulations consist of minimising the lateral displacement and orientation errors. A double lane-change manoeuvre was performed during 30 seconds with the sampling period being 0.01 seconds and the nominal payload subject to uncertainties. [Fig. 3](#) shows the scenario of studied cases, where e is the tractor width. Furthermore, [Table 3](#) shows the vehicle parameters and the necessary information to calculate it, obtained from websites for commercial vehicles¹ and towing implement² manufacturers. For all cases, the initial conditions are the

¹<https://www.scania.com>

²<http://www.librelato.com.br>

same, those being $x_0 = [0, 0, 0, 0, 0.3, -0.1]^T$, the penalty parameter $\mu = 10^8$,

$$H = \begin{bmatrix} 1 \\ 1 \\ 1 \\ 1 \\ 1 \\ 1 \\ 1 \end{bmatrix}, E_F = \begin{bmatrix} 6.8572 \times 10^{-5} \\ -8.6201 \times 10^{-5} \\ -2.1440 \times 10^{-5} \\ -10.4924 \times 10^{-5} \\ 0 \\ 666.66667 \times 10^{-5} \end{bmatrix}^T \text{ and } E_G = \begin{bmatrix} 666.66667 \times 10^{-5} \\ 666.66667 \times 10^{-5} \end{bmatrix}^T.$$

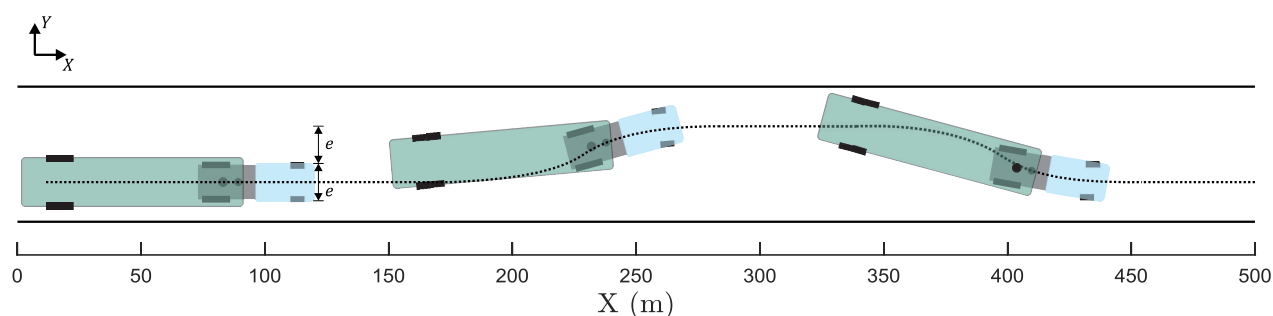


Figure 3: Double lane change scenario.

Table 3: Vehicle parameters values

Parameter	Meaning	Value
a_1	Distance from the front axle to the tractor centre of gravity	1.734 m
a_2	Distance from the coupling point to the trailer centre of gravity	4.8 m
b_1	Distance from the tractor rear axle to the tractor centre of gravity	2.415 m
b_2	Distance from the trailer axle to the trailer centre of gravity	3.2 m
l_1	Tractor wheelbase	4.149 m
l_2	Trailer wheelbase	8.0 m
d_1	The distance between the tractor rear axle and the coupling point	-0.29 m
h_1	The distance between coupling point and the tractor centre of gravity	2.125 m
l_1^*	The distance between the tractor front axle and the coupling point	3.859 m
e	Tractor width	2.6 m
v	Forward velocity	16.667 m/s
m_1	Tractor mass	8909 kg
m_2	Trailer mass	9370 kg
Payload	The amount of payload carried by the vehicle	24000 kg
J_1	Tractor moment of inertia	41566 kg m ²
J_2	Trailer moment of inertia	404360 kg m ²
c_1	Tractor front axle cornering stiffness	345155 N/rad
c_2	Tractor rear axle cornering stiffness	927126 N/rad
c_3	Trailer axle cornering stiffness	1158008 N/rad

The normalised cornering stiffness was applied in all cases studied here as it is a satisfactory representation for most applications and conditions [29]. Thus, it was calculated as a function of vertical load by assuming $f = f_1 = f_2 = f_3 = 5.73 \text{ rad}^{-1}$. In addition, the maximum steering angle (0.44 rad) was taken into account in numerical results.

The linear system must be rewritten in order to compare the \mathcal{H}_∞ control and the robust recursive regulator presented in this paper. Hence, the robust control design considering the \mathcal{H}_∞ method discussed by Hassib *et al.* [33] was used. Its equations, identifications and formulation are given in Appendix A.

Fig. 4 gives the block diagrams for both control techniques, where e_i is the error between the reference and output, and x_{ref} is the reference state vector. Both e_i and x_{ref} are obtained when a reference control signal is applied to the lateral model of the vehicle.

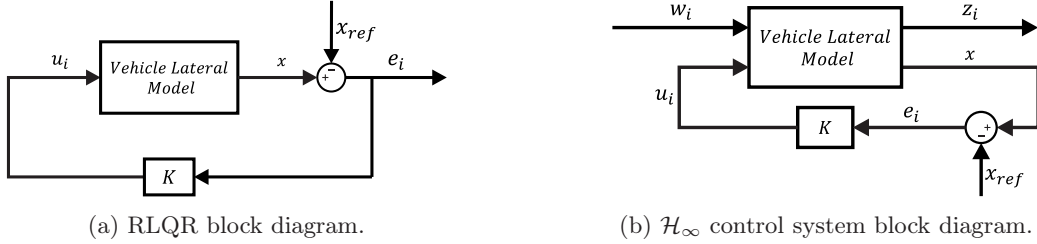


Figure 4: Block diagrams for Robust Linear Quadratic Regulator and \mathcal{H}_∞ control systems.

4.1. System response

The articulated heavy vehicle behaviour was evaluated with numerical results by taking a given reference path. For this purpose, the lateral velocity, yaw rate, articulation angle rate, articulation angle, lateral displacement and orientation error of the vehicle were observed. Moreover, controller evaluation was done through graphic analysis, and by adopting maximum steering rate and \mathcal{L}_2 norm of the error as performance criteria.

Table 4 and Table 5 show maximum steering rate, payload variations, and \mathcal{L}_2 norm of lateral displacement and orientation errors for both performed controllers, respectively. Payload values for every evaluated case were chosen for the best illustration of the influence of mass variation.

Table 4: Evaluated cases for both controllers

Case	Payload	$max\ \dot{\alpha}_{RLQR}\ $	$max\ \dot{\alpha}_{\mathcal{H}_\infty}\ $
1	100%	0.3432 rad/s	4.3750 rad/s
2	234%	0.4130 rad/s	8.4404 rad/s
3	237%	0.4164 rad/s	9.2350 rad/s
4	0%	0.3333rad/s	4.5959 rad/s

Table 5: \mathcal{L}_2 norm of the lateral displacement and orientation errors

Case	$\ \rho\ _{\mathcal{L}_2}$		$\ \theta\ _{\mathcal{L}_2}$	
	RLQR	\mathcal{H}_∞	RLQR	\mathcal{H}_∞
1	0.3727	0.2004	0.1481	0.0692
2	0.3886	0.1651	0.1331	0.0793
3	0.3882	0.4055	0.1328	0.2594
4	0.3217	0.2348	0.1358	0.0778

The robustness parameter γ was adjusted to the lowest possible value that ensures both \mathcal{H}_∞ controller existence and driving smoothness. Moreover, the nominal payload was applied, and the weight matrices Q and R were adjusted so that the maximum steering rate was $max\|\dot{u}\|_{RLQR} \approx 0.3432 \text{ rad/s}$. In addition,

the correspondent matrices R^c and Q^c have the same values adjusted in Q and R , respectively. Hence, for every cases:

$$\gamma = 14350, \quad Q = R^c = \begin{bmatrix} 1 & 0 & 0 & 0 & 0 & 0 \\ 0 & 1 & 0 & 0 & 0 & 0 \\ 0 & 0 & 1 & 0 & 0 & 0 \\ 0 & 0 & 0 & 1 & 0 & 0 \\ 0 & 0 & 0 & 0 & 25000 & 0 \\ 0 & 0 & 0 & 0 & 0 & 100 \end{bmatrix} \quad \text{and} \quad R = Q^c = \begin{bmatrix} 67070 & 0 \\ 0 & 67070 \end{bmatrix}.$$

Graphics of numerical results for each evaluated case and their case description follows.

Case 1 Considering nominal payload, Fig. 5 and Fig. 6 show the system state variables, the global position of tractor centre of mass and steering angle performed by both controllers.

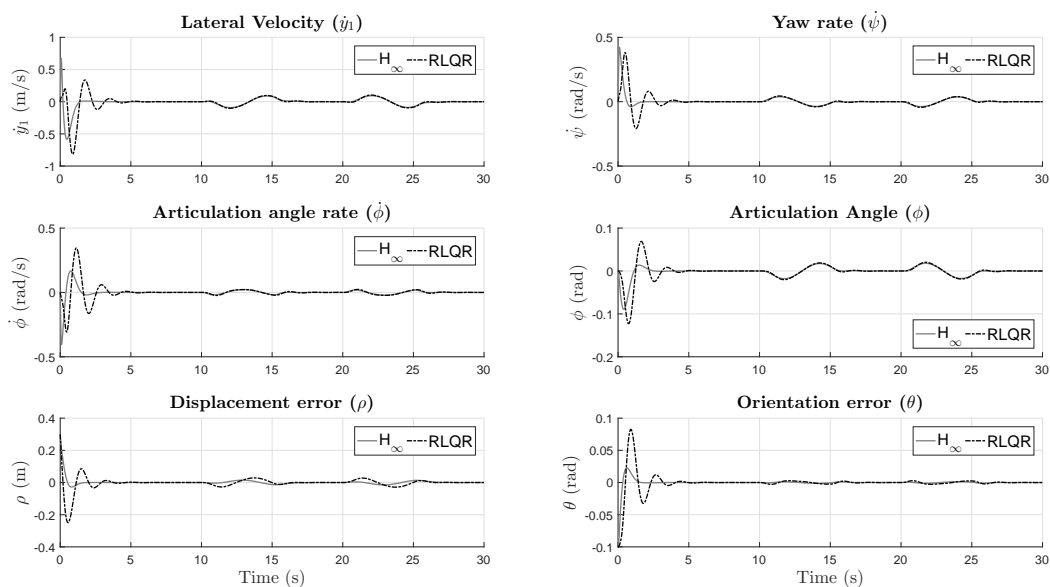


Figure 5: System state variables for case 1.

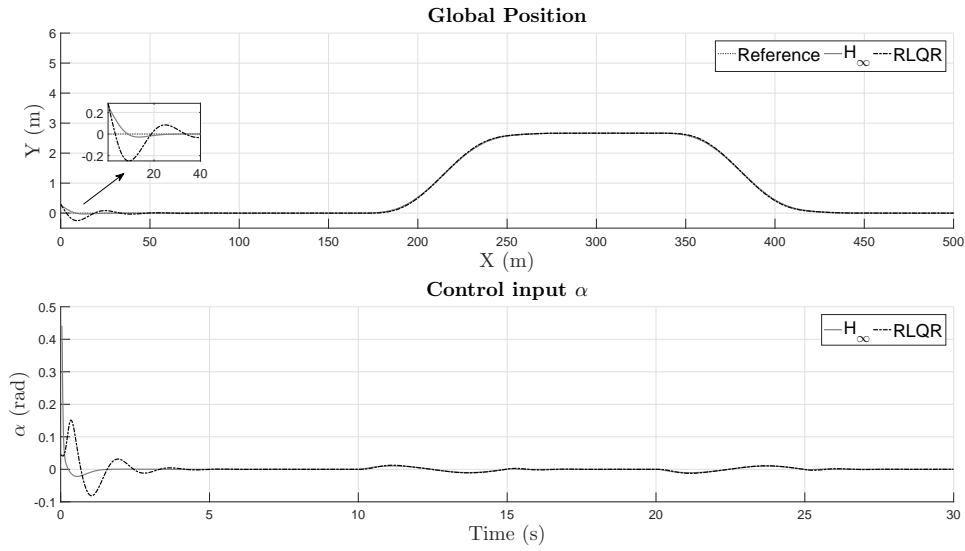


Figure 6: Global position of the tractor centre of mass and steering angle for case 1.

Case 2 Considering 234% of overload over the payload nominal value, Fig. 7 and Fig. 8 show the system state variables, the global position of tractor centre of mass and steering angle performed by both controllers.

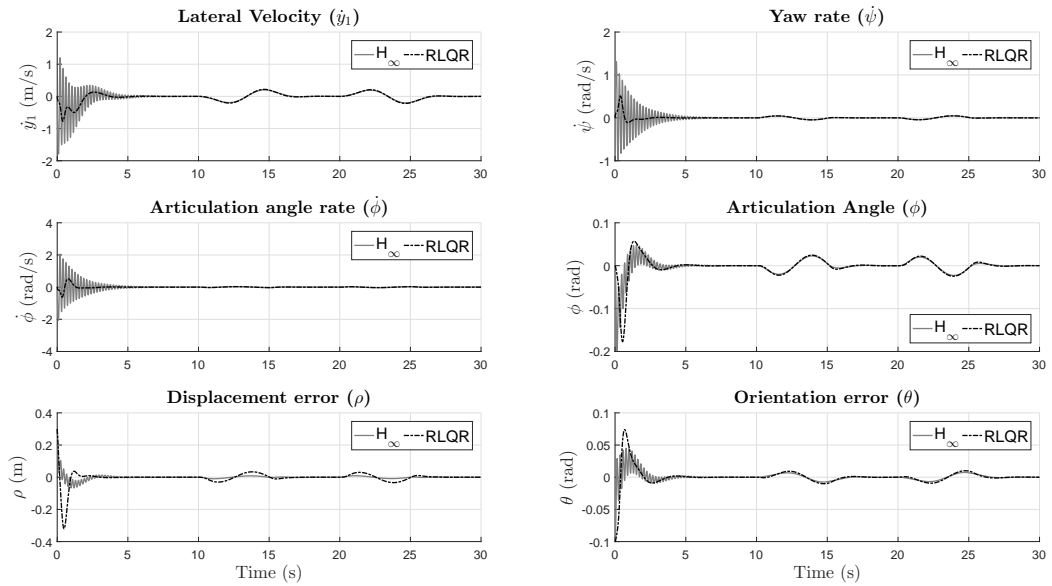


Figure 7: System state variables for case 2.

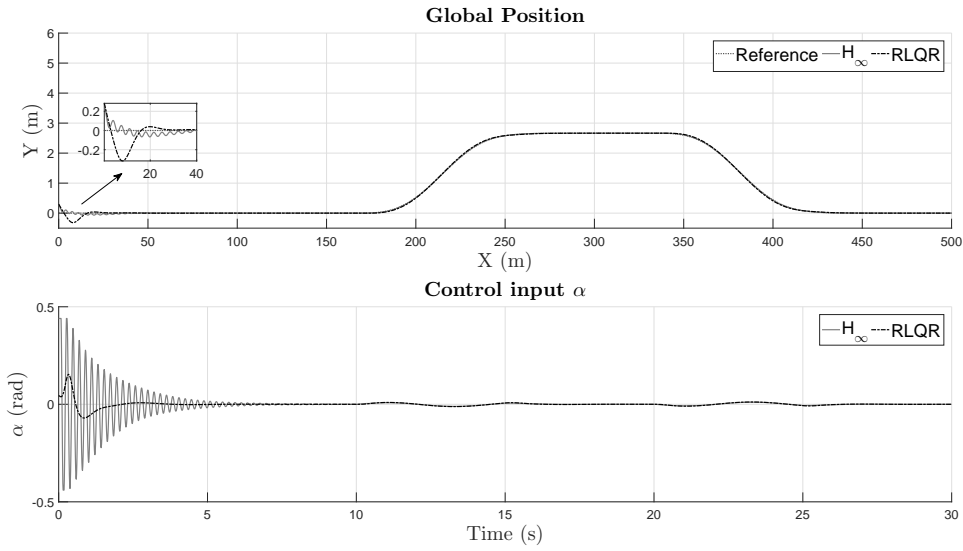


Figure 8: Global position of the tractor centre of mass and steering angle for case 2.

Case 3 Considering 237% of overload over the payload nominal value, Fig. 9 and Fig. 10 show the system state variables, the global position of tractor centre of mass and steering angle performed by both controllers.

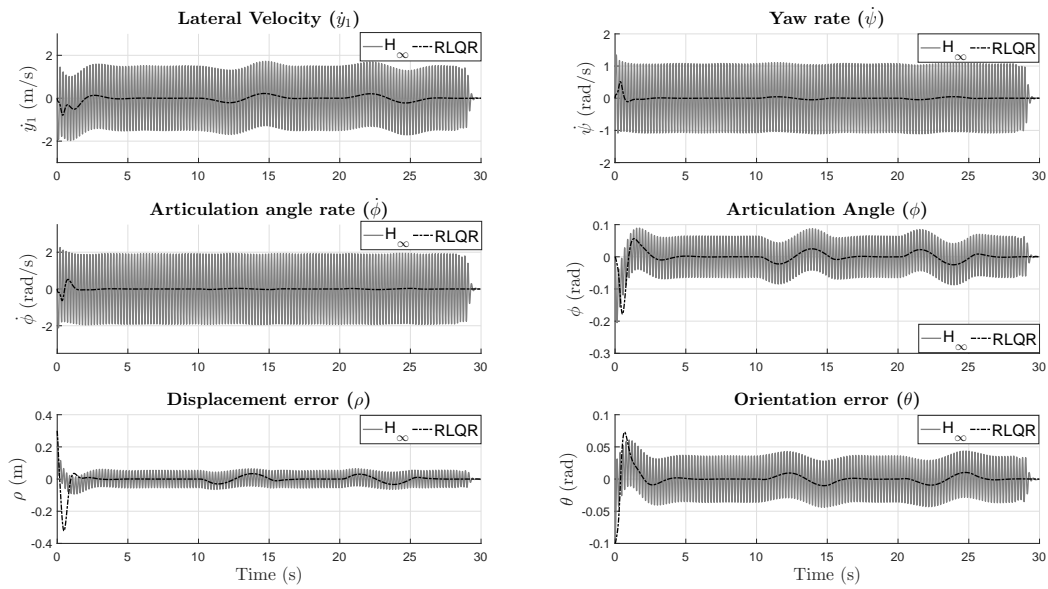


Figure 9: System state variables for case 3.

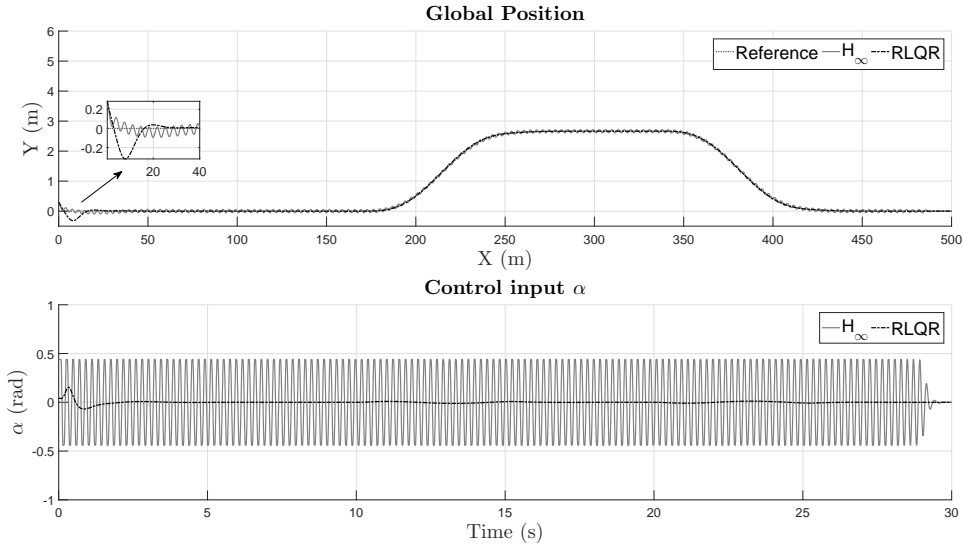


Figure 10: Global position of the tractor centre of mass and steering angle for case 3.

Case 4 Lastly, considering a vehicle without payload, Fig. 11 and Fig. 12 show the system state variables, the global position of the tractor centre of mass and steering angle performed by both controller.

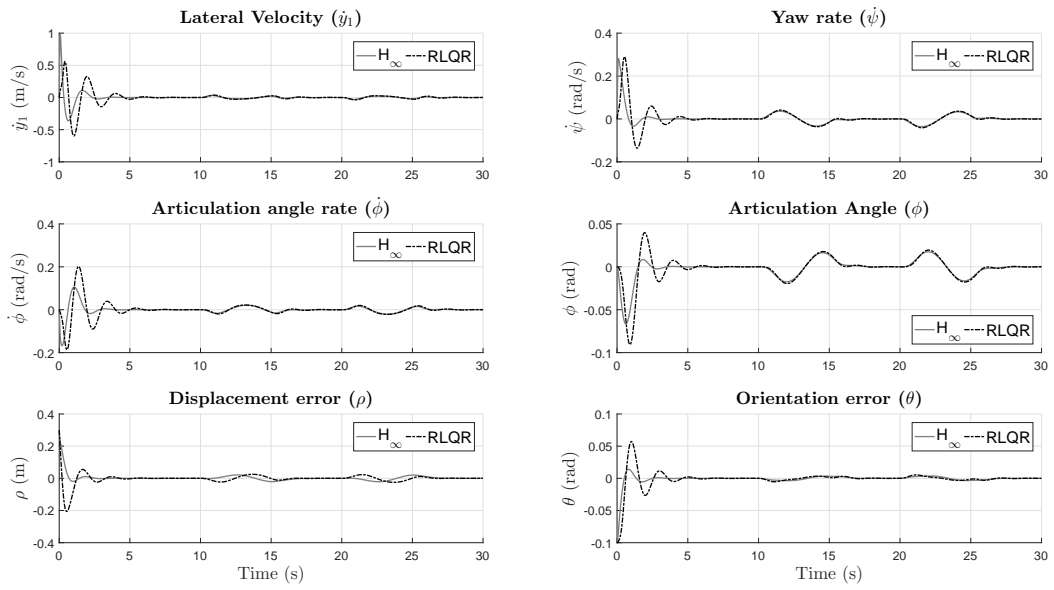


Figure 11: System state variables for case 4.

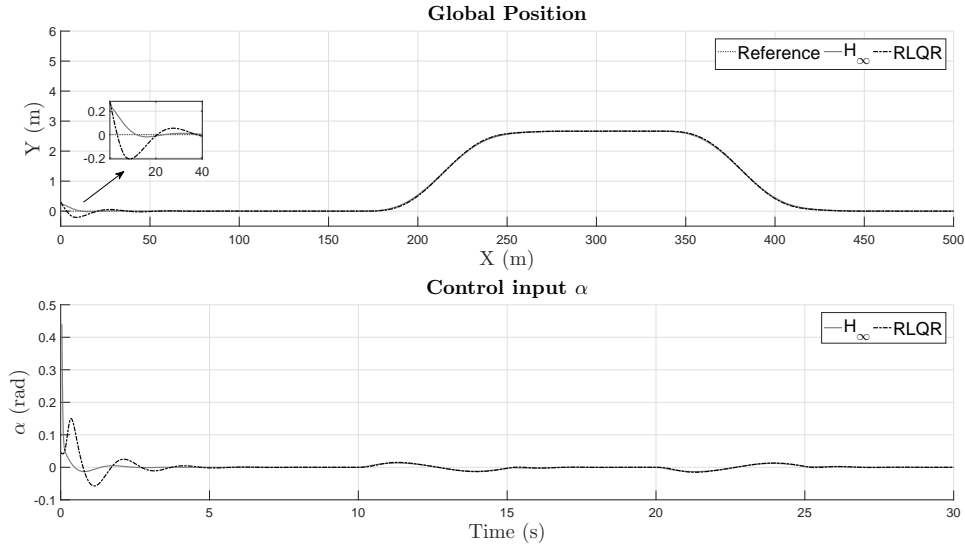


Figure 12: Global position of the tractor centre of mass and steering angle for case 4.

4.2. Discussion

The main goal of these evaluated cases was to show how the Robust Recursive Regulator deals with uncertainties in articulated heavy vehicles. Results demonstrate that the RLQR performance is less affected by payload mass variation than \mathcal{H}_∞ controller. It is verified in Table 5, where the \mathcal{L}_2 norm of the lateral displacement and orientation errors of the robust recursive regulator are less affected by mass uncertainties than \mathcal{H}_∞ controller.

Moreover, Table 4 shows that, in the presence of uncertainties, the $\max\|\dot{u}_{\mathcal{H}_\infty}\|$ is severely influenced by parametric variations while $\max\|\dot{u}_{RLQR}\|$ is much less affected. This is significant, since high steering angle rates mean abrupt driving, which may not be possible for the mechanical system of the vehicle, representing a safety limitation to the \mathcal{H}_∞ controller.

As shown in Fig. 5, Fig. 7, Fig. 9 and Fig. 11, the performed results for tractor lateral velocity \dot{y}_1 , tractor yaw rate $\dot{\psi}$, articulation angle rate $\dot{\phi}$ and articulation angle ϕ demonstrate that the robust recursive regulator deals better with vehicle lateral dynamic behaviour since its performance is much less affected by mass variations. Furthermore, the results obtained in Table 4 and Table 5 are shown in Fig. 5-12, confirming that the RLQR is still more robust, more stable, smoother and safer than \mathcal{H}_∞ in the presence of payload variations. For better performance of the \mathcal{H}_∞ controller, the parameter γ needs to be adjusted offline for each particular payload. This is very inefficient for practical applications given the wide mass variation in heavy-duty vehicles. The advantage of the RLQR is that does not require offline adjustment of auxiliary parameters, maintaining good performance for each evaluated case.

5. Conclusions

The Robust Linear Quadratic Regulator has been applied to perform the lateral control of an autonomous articulated heavy-duty vehicle subject to parametric uncertainties. Considering uncertainty in the towed mass, RLQR controller performance was better in terms of robustness, lateral stability, driving smoothness and safety when compared to \mathcal{H}_∞ robust control technique. Thus, the robust recursive regulator was demonstrated as a profitable control technique to deal with parametric uncertainties in such vehicle systems. The RLQ controller performs well for a wide range of payloads, while the performance of the \mathcal{H}_∞ controller is significantly affected by higher payloads, given a constant γ . Nevertheless, vertical and roll stability cannot be guaranteed because a model-based control design that only considers planar motion was used.

The robust recursive regulator could be exploited in non-articulated and multi-articulated vehicles in order to perform the path-following and lateral control. For future work, the articulated vehicle system will be extended to three-dimensions representation and experimental results will be obtained.

6. Acknowledgements

The authors would like to thank Coordination for the Improvement of Higher Education Personnel (CAPES), São Paulo Research Foundation (FAPESP, grant #2014/50851-0) and Vale S.A. for the financial support.

References

References

- [1] N. Wu, W. Huang, Z. Song, X. Wu, Q. Zhang, S. Yao, *Adaptive dynamic preview control for autonomous vehicle trajectory following with D* in: 2015 IEEE Intelligent Vehicles Symposium (IV), IEEE, 2015, pp. 1012–1017. doi:10.1109/ivs.2015.7225817. URL <https://doi.org/10.1109/ivs.2015.7225817>
- [2] M. Fu, K. Zhang, Y. Yang, H. Zhu, M. Wang, *Collision-free and kinematically feasible path planning along a reference path for autonomous* in: 2015 IEEE Intelligent Vehicles Symposium (IV), IEEE, 2015, pp. 907–912. doi:10.1109/ivs.2015.7225800. URL <https://doi.org/10.1109/ivs.2015.7225800>
- [3] J. Shin, J. Huh, Y. Park, *Asymptotically stable path following for lateral motion of an unmanned ground vehicle*, Control Engineering Practice 40 (2015) 102–112. doi:10.1016/j.conengprac.2015.03.006. URL <https://doi.org/10.1016/j.conengprac.2015.03.006>
- [4] C. M. Filho, M. H. Terra, D. F. Wolf, *Safe optimization of highway traffic with robust model predictive control-based cooperative adaptive c* IEEE Transactions on Intelligent Transportation Systems 18 (11) (2017) 3193–3203. doi:10.1109/tits.2017.2679098. URL <https://doi.org/10.1109/tits.2017.2679098>
- [5] J. E. A. Dias, G. A. S. Pereira, R. M. Palhares, *Longitudinal model identification and velocity control of an autonomous car*, IEEE Transactions on Intelligent Transportation Systems (2014) 1–11 doi:10.1109/tits.2014.2341491. URL <https://doi.org/10.1109/tits.2014.2341491>
- [6] M. S. Kati, H. Koroğlu, J. Fredriksson, *Robust lateral control of an a-double combination via \mathcal{H}_∞ and generalized \mathcal{H}_2 static output feedback* IFAC-PapersOnLine 49 (11) (2016) 305–311. doi:10.1016/j.ifacol.2016.08.046. URL <https://doi.org/10.1016/j.ifacol.2016.08.046>
- [7] B. A. Ujnovich, D. Cebon, *Path-following steering control for articulated vehicles*, Journal of Dynamic Systems, Measurement, and Control 135 (3) (2013) 031006. doi:10.1115/1.4023396. URL <https://doi.org/10.1115/1.4023396>
- [8] M. M. Islam, L. Laine, B. Jacobson, *Improve safety by optimal steering control of a converter dolly using particle swarm optimization for lo* in: 2015 IEEE 18th International Conference on Intelligent Transportation Systems, IEEE, 2015, pp. 2370–2377. doi:10.1109/itsc.2015.383. URL <https://doi.org/10.1109/itsc.2015.383>
- [9] D. J. Fagnant, K. Kockelman, *Preparing a nation for autonomous vehicles: opportunities, barriers and policy recommendations*, Transportation Research Part A: Policy and Practice 77 (2015) 167–181. doi:10.1016/j.tra.2015.04.003. URL <https://doi.org/10.1016/j.tra.2015.04.003>
- [10] H. Noorvand, G. Karnati, B. S. Underwood, *Autonomous vehicles*, Transportation Research Record: Journal of the Transportation Research Board 2640 (2017) 21–28. doi:10.3141/2640-03. URL <https://doi.org/10.3141/2640-03>
- [11] E. Alcalá, V. Puig, J. Quevedo, T. Escobet, R. Comasolivas, *Autonomous vehicle control using a kinematic lyapunov-based technique with I* Control Engineering Practice 73 (2018) 1–12. doi:10.1016/j.conengprac.2017.12.004. URL <https://doi.org/10.1016/j.conengprac.2017.12.004>
- [12] X. Ji, X. He, C. Lv, Y. Liu, J. Wu, *Adaptive-neural-network-based robust lateral motion control for autonomous vehicle at driving limits*, Control Engineering Practice 76 (2018) 41–53. doi:10.1016/j.conengprac.2018.04.007. URL <https://doi.org/10.1016/j.conengprac.2018.04.007>
- [13] I. Matraji, A. Al-Durra, A. Haryono, K. Al-Wahedi, M. Abou-Khousa, *Trajectory tracking control of skid-steered mobile robot based on ada* Control Engineering Practice 72 (2018) 167–176. doi:10.1016/j.conengprac.2017.11.009. URL <https://doi.org/10.1016/j.conengprac.2017.11.009>
- [14] Z. Chu, Y. Sun, C. Wu, N. Sepehri, *Active disturbance rejection control applied to automated steering for lane keeping in autonomous vehic* Control Engineering Practice 74 (2018) 13–21. doi:10.1016/j.conengprac.2018.02.002. URL <https://doi.org/10.1016/j.conengprac.2018.02.002>
- [15] C. Hu, H. Jing, R. Wang, F. Yan, M. Chadli, *Robust \mathcal{H}_∞ output-feedback control for path following of autonomous ground vehicles*, Mechanical Systems and Signal Processing 70-71 (2016) 414–427. doi:10.1016/j.ymsp.2015.09.017. URL <https://doi.org/10.1016/j.ymsp.2015.09.017>

- [16] K.-i. Kim, H. Guan, B. Wang, R. Guo, F. Liang, *Active steering control strategy for articulated vehicles*, *Frontiers of Information Technology & Electronic Engineering* 17 (6) (2016) 576–586. doi:10.1631/FITEE.1500211. URL <https://doi.org/10.1631/FITEE.1500211>
- [17] H. Guan, K. Kim, B. Wang, *Comprehensive path and attitude control of articulated vehicles for varying vehicle conditions*, *International Journal of Heavy Vehicle Systems* 24 (1) (2017) 65. doi:10.1504/ijhvs.2017.080961. URL <https://doi.org/10.1504/ijhvs.2017.080961>
- [18] H. Yuan, H. Zhu, *Anti-jackknife reverse tracking control of articulated vehicles in the presence of actuator saturation*, *Vehicle System Dynamics* 54 (10) (2016) 1428–1447. arXiv:<https://doi.org/10.1080/00423114.2016.1208251>, doi:10.1080/00423114.2016.1208251. URL <https://doi.org/10.1080/00423114.2016.1208251>
- [19] M. M. Michalek, *A highly scalable path-following controller for n-trailers with off-axle hitching*, *Control Engineering Practice* 29 (2014) 61–73. doi:10.1016/j.conengprac.2014.04.001. URL <https://doi.org/10.1016/j.conengprac.2014.04.001>
- [20] T. Nayl, G. Nikolakopoulos, T. Gustafsson, D. Kominiak, R. Nyberg, *Design and experimental evaluation of a novel sliding mode controller*, *Robotics and Autonomous Systems* 103 (2018) 213–221. doi:10.1016/j.robot.2018.01.006. URL <https://doi.org/10.1016/j.robot.2018.01.006>
- [21] M. H. Terra, J. P. Cerri, J. Y. Ishihara, *Optimal robust linear quadratic regulator for systems subject to uncertainties*, *IEEE Transactions on Automatic Control* 59 (9) (2014) 2586–2591. doi:10.1109/tac.2014.2309282. URL <https://doi.org/10.1109/tac.2014.2309282>
- [22] J. P. Cerri, M. H. Terra, J. Y. Ishihara, *Recursive robust regulator for discrete-time state-space systems*, in: 2009 American Control Conference, IEEE, 2009, pp. 3077–3082. doi:10.1109/acc.2009.5160553. URL <https://doi.org/10.1109/acc.2009.5160553>
- [23] C. Li, H. Jing, R. Wang, N. Chen, *Vehicle lateral motion regulation under unreliable communication links based on robust \mathcal{H}_∞ output-feed*, *Mechanical Systems and Signal Processing* 104 (2018) 171 – 187. doi:<https://doi.org/10.1016/j.ymsp.2017.09.012>. URL <http://www.sciencedirect.com/science/article/pii/S0888327017304892>
- [24] W. Zhao, H. Zhang, Y. Li, *Displacement and force coupling control design for automotive active front steering system*, *Mechanical Systems and Signal Processing* 106 (2018) 76 – 93. doi:<https://doi.org/10.1016/j.ymsp.2017.12.037>. URL <http://www.sciencedirect.com/science/article/pii/S0888327017306751>
- [25] R. Skjetne, T. Fossen, *Nonlinear maneuvering and control of ships*, in: MTS/IEEE Oceans 2001. An Ocean Odyssey. Conference Proceedings (IEEE Cat. No.01CH37295), Vol. 3, Marine Technol. Soc, 2001, pp. 1808–1815. doi:10.1109/oceans.2001.968121. URL <https://doi.org/10.1109/oceans.2001.968121>
- [26] D. Schramm, M. Hiller, R. Bardini, *Vehicle Dynamics*, Springer Berlin Heidelberg, 2018. doi:10.1007/978-3-662-54483-9. URL <https://doi.org/10.1007/978-3-662-54483-9>
- [27] M. F. van de Molengraft-Luijten, I. J. Besselink, R. M. Verschuren, H. Nijmeijer, *Analysis of the lateral dynamic behaviour of articulated commercial vehicles*, *Vehicle System Dynamics* 50 (sup1) (2012) 169–189. doi:10.1080/00423114.2012.676650. URL <https://doi.org/10.1080/00423114.2012.676650>
- [28] P. S. Fancher, *Directional dynamics considerations for multi-articulated, multi-axled heavy vehicles*, in: SAE Technical Paper Series, SAE International, 1989, pp. 630–640. doi:10.4271/892499. URL <https://doi.org/10.4271/892499>
- [29] M. Luijten, *Lateral dynamic behaviour of articulated commercial vehicles*, Eindhoven University of Technology.
- [30] L. Houben, *Analysis of truck steering behaviour using a multi-body model*, Master’s thesis, Eindhoven University of Technology, DCT 343.
- [31] T. Kailath, A. H. Sayed, B. Hassibi, *Linear Estimation*, Prentice Hall, New Jersey, 2000.
- [32] A. H. Sayed, V. H. Nascimento, *Design criteria for uncertain models with structured and unstructured uncertainties*, in: *Robustness in identification and control*, Springer London, 1999, pp. 159–173. doi:10.1007/bfb0109867. URL <https://doi.org/10.1007/bfb0109867>
- [33] B. Hassibi, A. H. Sayed, T. Kailath, *Indefinite-Quadratic Estimation and Control*, Society for Industrial and Applied Mathematics, 1999. doi:10.1137/1.9781611970760. URL <https://doi.org/10.1137/1.9781611970760>

Appendix A. \mathcal{H}_∞ control

The robust control design considering \mathcal{H}_∞ method mentioned in [33] is used for the following linear system

$$x_{i+1} = F_i + G_{1,i}w_i + G_{2,i}u_i, \quad i = 0, \dots, N, \quad (\text{A.1})$$

where x_i is the state vector, u_i is the control input and w_i is the disturbance. In its sub-optimal formulation, this technique is based on finding a control strategy where for every x_0 and $\{w_i\}_{i=0}^N$,

$$\frac{x_{N+1}^{*T} P_{N+1}^c x_{N+1}^* + \sum_{i=0}^N (u_i^{*T} Q_i^c u_i^* + x_i^{*T} R_i^c x_i^*)}{x_0^{*T} \Pi_0^{-1} x_0^* + \sum_{i=0}^N (w_i^{*T} Q_i^w w_i^*)} < \gamma^2, \quad (\text{A.2})$$

for a suitable $\gamma > 0$, where P_{N+1}^c , Q_i^c , R_i^c , Π_0 and Q_i^w are non-negative definite weighing matrices. Such matrices are associated with the final state, control input, state, initial state and disturbance, respectively. The recursive solution of this problem is formulated in terms of backwards Riccati equation and the verification of some existence conditions is necessary.

To perform the control using this technique, uncertain system (7)-(8) must be rewritten as the system (A.1). Hence, the following immediate identifications are considered

$$\begin{aligned} F_i &\leftarrow F_i, \quad G_{2,i} \leftarrow G_i \quad x_i \leftarrow x_i, \quad u_i \leftarrow u_i, \quad G_{1,i} \leftarrow H_i, \quad w_i \leftarrow \Delta_i \begin{bmatrix} E_{F_i} & E_{G_i} \end{bmatrix} \begin{bmatrix} x_i \\ u_i \end{bmatrix}, \\ P_{N+1}^c &\leftarrow P_{N+1}, \quad Q_i^c \leftarrow R_i, \quad R_i^c \leftarrow Q_i, \quad Q_i^w \leftarrow I, \quad \Pi_0 \leftarrow I. \end{aligned} \quad (\text{A.3})$$

In order to use the system (A.1) as the uncertain system (7)-(8), some algebraic manipulations are necessary. Considering $R_{G,i}^c{}^{-1} = Q_i^c + G_{2,i}^T P_{N+1}^c G_{2,i}$, the control signal is obtained from [33] as

$$\begin{aligned} u_i &= -R_{G,i}^c{}^{-1} G_{2,i}^T P_{N+1}^c F_i x_i - R_{G,i}^c{}^{-1} G_{2,i}^T P_{N+1}^c G_{1,i} w_i \\ &= (-R_{G,i}^c{}^{-1} G_{2,i}^T P_{N+1}^c) (F_i x_i + G_{1,i} w_i). \end{aligned} \quad (\text{A.4})$$

From identifications made in (A.3) substitutions can be made in $G_{1,i}$ and w_i

$$\begin{aligned} u_i &= (-R_{G,i}^c{}^{-1} G_{2,i}^T P_{N+1}^c) ((F_i + H_i \Delta E_{F_i}) x_i + H_i \Delta E_{G_i} u_{i-1}) \\ &= -R_{G,i}^c{}^{-1} G_{2,i}^T P_{N+1}^c (F_i + \delta F_i) x_i - R_{G,i}^c{}^{-1} G_{2,i}^T P_{N+1}^c H_i \Delta E_{G_i} u_{i-1}, \end{aligned}$$

and adding G_2 in both sides of the equation the (A.4) becomes

$$\begin{aligned} u_i &= -R_{G,i}^c{}^{-1} G_{2,i}^T P_{N+1}^c (F_i + \delta F_i) x_i - R_{G,i}^c{}^{-1} G_{2,i}^T P_{N+1}^c (G_{2,i} + H_i \Delta E_{G_i}) u_{i-1} + R_{G,i}^c{}^{-1} G_{2,i}^T P_{N+1}^c G_{2,i} u_{i-1} \\ &= -R_{G,i}^c{}^{-1} G_{2,i}^T P_{N+1}^c (F_i + \delta F_i) x_i - R_{G,i}^c{}^{-1} G_{2,i}^T P_{N+1}^c (G_{2,i} + \delta G_{2,i}) u_{i-1} + R_{G,i}^c{}^{-1} G_{2,i}^T P_{N+1}^c G_{2,i} u_{i-1}. \end{aligned} \quad (\text{A.5})$$

Considering the sampling period sufficiently small so that $x_i \approx x_{i-1}$, the (A.5) can be rewritten as

$$u_i := -R_{G,i}^c{}^{-1} G_{2,i}^T P_{N+1}^c ((F_i + \delta F_i) x_{i-1} + (G_{2,i} + \delta G_{2,i}) u_{i-1}) + R_{G,i}^c{}^{-1} G_{2,i}^T P_{N+1}^c G_{2,i} u_{i-1}.$$

Thus, as $u_{i-1} = z_i$, the system (A.1) can be rewritten as system (7)-(8)

$$\begin{aligned} x_{i+1} &= (F_i + \delta F_i) x_i + (G_{2,i} + \delta G_{2,i}) u_i \\ \begin{bmatrix} \delta F_i & \delta G_i \end{bmatrix} &= H_i \Delta_i \begin{bmatrix} E_{F_i} & E_{G_i} \end{bmatrix}, \end{aligned}$$

where

$$u_i = -R_{G,i}^c{}^{-1} G_{2,i}^T P_{N+1}^c x_i + R_{G,i}^c{}^{-1} G_{2,i}^T P_{N+1}^c G_{2,i} z_i. \quad (\text{A.6})$$

See details in [33].